ARTICLE NO. 79-0883R

A80-077

10022
60004
70024

Inductive Energy Storage for MPD Thrusters

L. K. Rudolph* and R. M. Jones†
Jet Propulsion Laboratory, California Institute of Technology, Pasadena, Calif.

The high thrust density of the self-field magnetoplasmadynamic thruster makes it a promising candidate for many advanced space missions. The high power requirements of this thruster lead to its operation in a pulsed mode from an energy storage device. The system characteristics of an inductive energy storage circuit with solar array power from 25 to 375 kW are considered by solving the circuit equations for the inductor charge and discharge phases. Using simple analytic models of the circuit components, the total system efficiency and inductance are determined as functions of the array output power and circuit resistance. The total system efficiency increases with array power and is acceptable only for low values of circuit resistance, indicating that superconducting circuitry should be investigated. The inductor mass scales inversely with solar array power such that at lower powers, capacitive storage may be more desirable.

Nomenclature

E_{ch} = energy supplied by the solar array during the charging phase, kJ
E_{dis} = energy supplied by the solar array during the discharge phase, kJ
E_{MPD} = energy used by the thruster during the discharge phase, kJ
J_{ch} = circuit current during the charging phase, kA
J = circuit current during the discharge phase, kA
J_{max} = maximum circuit current, kA
J_{min} = minimum circuit current, kA
J_{arr} = current through the solar array, kA
J^* = thruster onset current, kA
L = total circuit inductance, mH
P_{arr} = power supplied by the solar array, kW
q = discharge phase equation discriminant, $(m\Omega)^2$
R = total circuit resistance, mΩ
t = time, s
T = circuit charging time, s
ΔT = circuit discharge time, s
V_F = MPD thruster electrode fall voltage, V
V = voltage across the thruster electrodes, V
V_{arr} = voltage across the solar array, V
α = MPD thruster efficiency-current coefficient, $(kA)^{-1}$
β = MPD thruster voltage-current coefficient, $V/(kA)^2$
γ = solar array voltage-current coefficient, V/kA
ζ = solar array open circuit voltage, V
η = total system efficiency
η_{MPD} = MPD thruster efficiency
θ = MPD thruster efficiency, zero current intercept

Introduction

THE self-field magnetoplasmadynamic (MPD) thruster is an attractive candidate for application on a variety of future space missions which require relatively high thrust densities at specific impulses greater than 1000 s. The inferred efficiency at specific impulses less than 5000 s, and the relative simplicity of this type of thruster system, offer substantial benefits for near-Earth orbit-to-orbit transport. Furthermore, with potential improvements in efficiency at higher specific impulses, the trip times for high-power outer planet exploration may be reduced.

The MPD thruster accelerates a neutral plasma by Lorentz forces induced through a high-current discharge interaction with its self-magnetic field.[1] The resulting thrust scales approximately with the square of the discharge current, while the losses scale more linearly; hence, it is advantageous to operate this device at as high a discharge current as possible consistent with system limits.[2,3] The thrust, efficiency, and specific impulse increase with increasing discharge current up to megawatt input power levels. This increase in MPD thruster performance with discharge power is so strong, that for power levels presently under study, it is advantageous to operate the thruster in a quasisteady mode from an energy storage system that provides megawatt power levels in long pulses via an on-off duty cycle.[4]

Future application of the MPD thruster system may occur on spacecraft with either nuclear or solar power systems. In addition, various energy storage devices for MPD thrusters can be envisioned, including capacitive, inductive, and inertial systems. In order to determine the particular advantages and disadvantages of these alternatives for various steady-state power levels, an ongoing program has begun to examine the characteristics of an MPD thruster system using these various types of energy storage devices and power systems.In this report, the calculated characteristics of an inductive energy storage-MPD thruster system are presented. Previous studies have examined the operation of such a system powered by a 400 kW nuclear thermionic generator[5,6]; however, little study has been devoted to the variation of the system characteristics with input power supply type and level. The studies of this report were carried out for a solar array with power levels of 25, 100, and 375 kW to determine the variation of an inductive storage system with power and to facilitate an eventual comparison between nuclear thermionic and solar cell power systems. The results of these studies indicate that the variation in MPD thruster efficiency plays a major role in determining the optimum operation of the MPD thruster-inductor system. In addition, as previously expected, these studies show inductive storage is more suitable for high-power systems, due to an increasing ratio of resistive losses to input power associated with lower power operation.

System Circuit Model

The MPD thruster-inductive energy storage circuit chosen for consideration in this study is shown in Fig. 1. It consists of a solar array power supply in series with an energy storage coil L and an MPD thruster. The internal resistance of the inductor and the series resistance of the solar array current leads are combined into one equivalent resistance, R. The

Presented as Paper 79-0883 at the AIAA/NASA Conference on Advanced Technology for Future Space Systems, Hampton, Va., May 8-11, 1979; submitted Sept. 25, 1979; revision received March 10, 1980. This paper is declared a work of the U.S. Government and therefore is in the public domain.

Index categories: Electric and Advanced Space Propulsion; Power Conditioning; Spacecraft Propulsion Systems Integration.

*Senior Engineer. Member AIAA.
†Engineer. Member AIAA.

thruster is in parallel with a switch that controls the inductor charging and discharging phases. For the purposes of this study, the switch is assumed to be ideal, in the sense that it has an infinite resistance when open, a zero resistance when closed, and an infinitely fast response time.

The conceptual operation of this circuit is outlined schematically in Fig. 2, which shows the charging current through the inductor and the discharge current through the MPD thruster, as functions of time from the inception of system operation. Initially, the switch is closed, as shown in Fig. 1a, and the power supply charges the inductor to its peak current J_{max}. The switch is then opened, as shown in Fig. 1b, for the first thruster discharge pulse, during which time the current decays to its minimum value J_{min}. When this discharge pulse is completed, the switch is closed and the inductor is recharged to the maximum current. This charge-discharge cycle is continually repeated for as long as the mission requires. The following analysis considers only the continuous charge-discharge cycle in terms of J_{max}, J_{min}, ΔT, and T, and neglects the initial start-up and final shut-down operation.

To evaluate the performance of the inductive storage circuit of Fig. 1, the voltage-current characteristics of the MPD thruster must be approximated analytically. It is well known that the voltage of the MPD thruster for a given current depends strongly on the thruster electrode design and propellant characteristics.[7] Although current thruster design and operation is far from optimum, recent work has led to the development of a thruster with performance characteristics of interest for future application.[8] This thruster has a voltage-current characteristic as shown in Fig. 3 for operation with argon propellant. In order to model this characteristic analytically in as simple a manner as possible, a quadratic equation was used. This equation, shown as the dashed line in Fig. 3, is

$$V=\beta J^2+V_F \tag{1}$$

where $V_F=20$ V and $\beta=0.34$ V-kA^{-2}. As can be seen, this expression fits the known characteristic to well within the experimental error.

As the discharge current in the MPD thruster is increased, an onset current is reached, above which erratic terminal voltage fluctuations and increasing insulator and electrode ablation are observed.[9,10] To avoid these undesirable performance characteristics, the maximum acceptable MPD discharge current is limited to values at or below this onset current. Since MPD thruster performance improves with increasing discharge current, the most desirable performance is at a current just equal to J^*. For the MPD thruster voltage-current characteristics of Fig. 3, $J^*=23$ kA. For the following system analysis, J_{max} will be taken to be equal to J^* in order to arrive at the most desirable MPD thruster performance.

The solar array voltage-current characteristic was built up by considering a series-parallel grouping of individual solar cells. Each cell has a typical voltage-current characteristic as shown in Fig. 4, with an open circuit voltage of 0.5 V and a maximum power of 106 mW at a voltage of 0.425 V and a current of 250 mA. To simplify the following analysis, this characteristic is approximated by a straight line connecting the maximum power point to the open-circuit voltage point as shown in Fig. 4. Although the error is relatively large for some areas of this curve, this approximation is conservative in the sense that it gives output powers that are lower than the real characteristic values.

The number of individual cells in the solar array is fixed by the maximum array output power P_{arr} and the maximum output power of each cell. In addition, the total number of series groupings of cells is fixed by J_{max} and the maximum cell current of 250 mA. Using the results of these calculations and the approximate cell voltage-current characteristic gives a

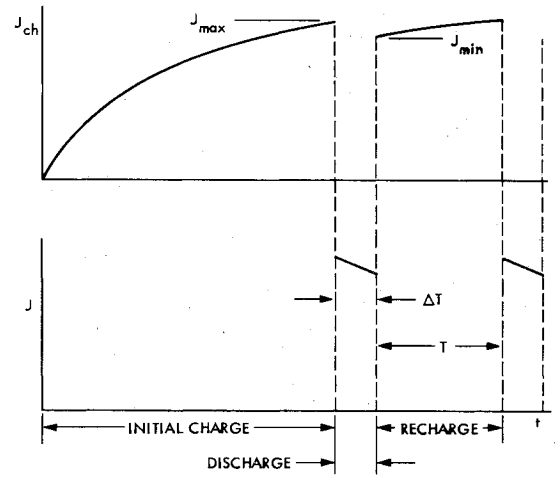

Fig. 2 Conceptual circuit operation.

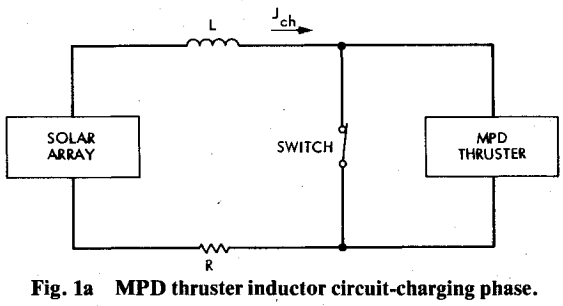

Fig. 1a MPD thruster inductor circuit-charging phase.

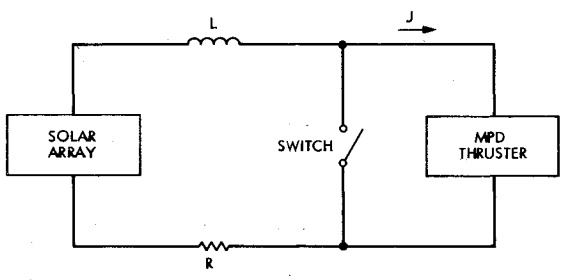

Fig. 1b MPD thruster inductor circuit-discharge phase.

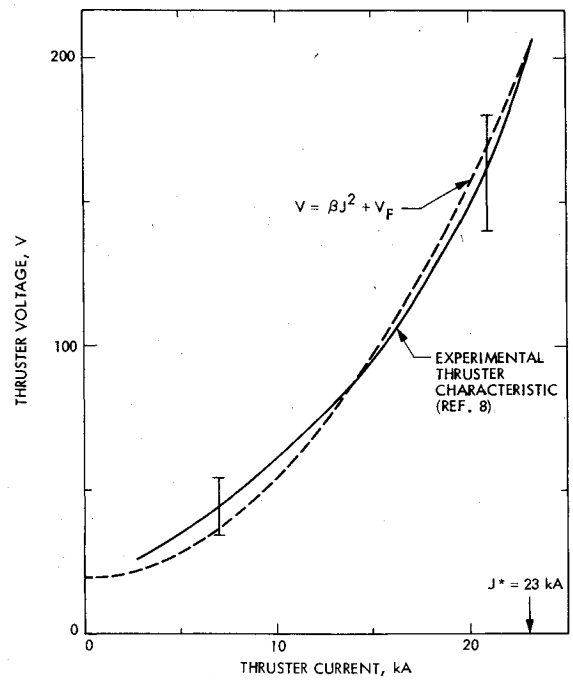

Fig. 3 Typical MPD voltage-current characteristic.

total array voltage-current characteristic of the form

$$V_{arr} = \gamma J_{arr} + \zeta \tag{2}$$

where

$$\gamma = -0.176\, P_{arr}/J_{max}^2 \qquad \zeta = 1.17\, P_{arr}/J_{max}$$

The value of P_{arr} will be varied in the analysis while, as previously noted, J_{max} will be set equal to J^*.

Having approximate analytic expressions for both the MPD thruster and solar array voltage-current characteristics, the basic equations describing the response of the inductive storage circuit can be developed. Two circuit equations are required—one for the inductor charging phase with the switch closed and one for the thruster discharge phase with the switch opened. These equations can be written as

$$-\gamma J_{ch} - \zeta + RJ_{ch} + L(dJ_{ch}/dt) = 0 \tag{3}$$

$$\gamma J + \zeta - JR - L(dJ/dt) - V_F - \beta J^2 = 0 \tag{4}$$

For each equation, time will be referenced to the beginning of the phase; hence, for the charging phase at time zero, the current is J_{min} and at time T, the current is J_{max} (see Fig. 2). For the discharge phase at time zero, the current is J_{max} and at time ΔT, the current is J_{min}. These boundary conditions tie the two equations together for a consistent solution.

The solution to the charging phase Eq. (3) is a simple rising exponential:

$$J_{ch}(t) = \frac{\zeta}{R-\gamma} - \left[\frac{\gamma}{R-\gamma} - J_{min}\right]\exp\left[\frac{(\gamma-R)t}{L}\right] \tag{5}$$

This equation identically satisfies the boundary condition that at time equal to zero the current equals J_{min}. The second boundary condition on this equation is that at time T the current must equal J_{max}. Substituting T and J_{max} into Eq. (5) gives an expression for T in terms of J_{min} and J_{max}:

$$T = \frac{L}{\gamma - R}\ln\left[\frac{J_{max} - \zeta/(R-\gamma)}{J_{min} - \zeta/(R-\gamma)}\right] \tag{6}$$

Since T is the time required to recharge the inductor from J_{min} to J_{max}, it must always be positive. This requirement leads to the criteria that

$$R < P_{arr}/J_{max}^2 \tag{7}$$

For the solar array powers considered in this report (25, 100, and 375 kW), this criteria restricts the total circuit resistance to values below 0.047 to 0.71 mΩ. These values imply that relatively massive current leads are required in the solar array and inductor configurations.

The discharge phase Eq. (4) can be rewritten as

$$L(dJ/dt) = -\beta J^2 + (\gamma - R)J + (\zeta + V_F) \tag{8}$$

The right-hand side of this equation is a quadratic expression for current with a discriminant

$$q = -4\beta(\zeta + V_F) - (\gamma - R)^2 \tag{9}$$

The algebraic form of the solution to Eq. (8) depends on the sign of this discriminant; thus, q must be evaluated as a function of solar array power and circuit resistance. For a given resistance, the value of power that makes q identically zero is shown as the solid line in Fig. 5. For powers below and to the left of this curve, q is positive, while for powers above and to the right, q is negative. Also shown in this figure is a dashed line representing the boundary of the inequality of Eq. (7), where acceptable operation is below and to the right. For the solar array powers under study in this report, the approximate operating regime is cross-hatched in Fig. 5, where q is positive.

Knowing the sign of the discriminant of Eq. (8), its solution can be written as

$$J(t) = \frac{-\sqrt{q}}{2\beta}\tan\left\{\frac{\sqrt{q}}{2L} + \tan^{-1}\left[\frac{(\gamma-R) - 2\beta J_{max}}{\sqrt{q}}\right]\right\} + \frac{(\gamma-R)}{2\beta} \tag{10}$$

This equation describes the decay of the discharge phase current from J_{max} at time equal to zero, to J_{min} at time ΔT. It identically satisfies the zero time condition and can be solved for the value of ΔT that yields J_{min}:

$$\Delta T = \frac{2L}{\sqrt{q}}\left\{\tan^{-1}\left[\frac{(\gamma-R) - 2\beta J_{min}}{\sqrt{q}}\right] - \tan^{-1}\left[\frac{(\gamma-R) - 2\beta J_{max}}{\sqrt{q}}\right]\right\} \tag{11}$$

This discharge time is positive definite as long as $J_{max} > J_{min}$.

Performance Analysis

Estimates of the MPD thruster system parameters can be made using the equations for the charge and discharge phases developed in the previous section. These characteristics, such as inductance and charging time, will be evaluated for various power levels, minimum currents, and resistance values. The circuit resistance will be varied from the maximum value given by Eq. (7) where the system power is all absorbed in Ohmic losses, to a value of zero, where the Ohmic loses are negligible. The minimum current will vary from zero to J_{max}. Ultimately, estimates of the total system efficiency will fix J_{min} to a particular value depending on circuit resistance.

The MPD discharge initial transient time prior to actual quasisteady operation is known to be approximately 10^{-4} s (Ref. 4) hence, for the discharge to be dominated by its quasisteady performance, the total discharge time should be of order or greater than 10^{-3} s. To determine the value of circuit inductance in terms of solar array power, circuit resistance, and discharge time, Eq. (11) can be solved for L. To find the minimum value of L for acceptable quasisteady operation, the discharge time will be taken to be just equal to 10^{-3} s. Once this value of inductance is determined, Eq. (6) can be used to calculate T as a function of power and resistance.

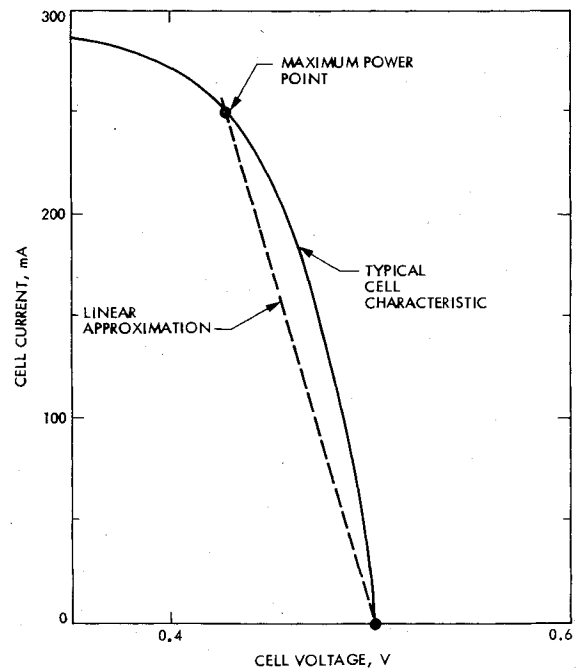

Fig. 4 Typical solar cell voltage-current characteristic.

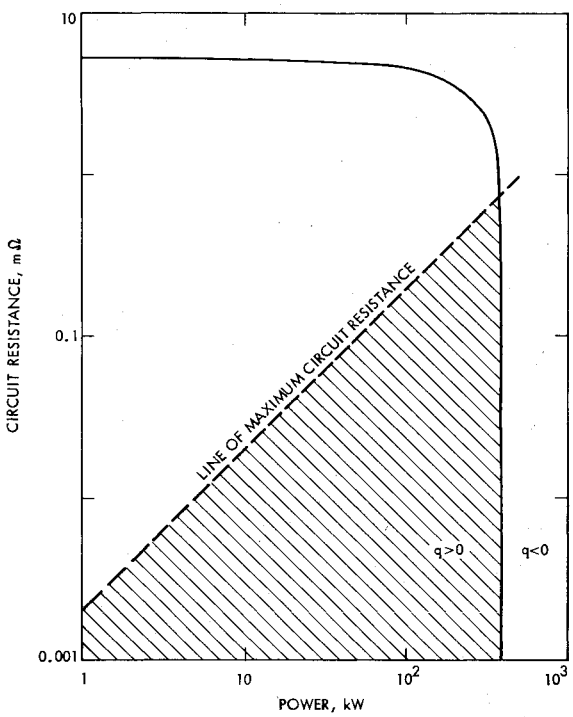

Fig. 5 Domain of circuit solution validity.

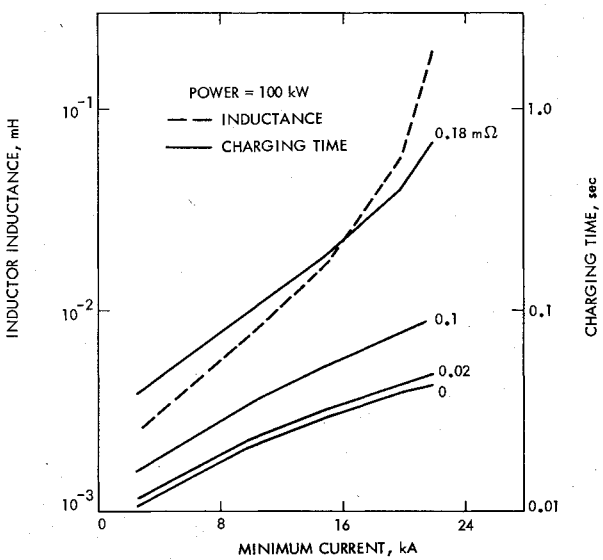

Fig. 6 Inductance and charging time for a fixed power.

The energy stored in the inductor must be sufficient to operate the MPD thruster and provide for resistive losses during the discharge phase. As J_{min} increases, the energy required to operate the thruster increases as does the energy dissipated in the resistor. The energy stored in the inductor during the charging phase is equal to $L(J_{max}^2 - J_{min}^2)/2$; thus, as this energy increases along with J_{min}, the inductance increases toward infinity. This effect is shown in Fig. 6, along with the increased charging time required by the increasing discharge energy for a given power. For a given value of J_{min}, the known increase in the required inductance with increasing resistance is too slight to be distinguished in this figure. The decreasing charging time with decreasing resistance is due to the drop in resistance losses during the charging phase and the corresponding increase in available power to charge the inductor.

Figure 7 shows the inductance and charging times for a given resistance and various power levels. As expected, larger powers lead to shorter charging times. In addition, the inductance is relatively insensitive to power, since it is determined primarily by the energy required in the discharge phase, and because the energy supplied during the discharge phase is small. The curve of inductance for a power of 100 kW has been omitted for clarity.

The MPD thrust efficiency is defined as the ratio of the directed kinetic energy appearing in the thrust to the energy supplied to the thruster electrodes. For the particular MPD thruster under consideration in this report,[8] this thrust efficiency depends on MPD discharge current as shown in Fig. 8. Again, it must be pointed out that the thruster under consideration is a laboratory model and far from optimized; hence, future development will have a strong impact on the thruster characteristics. To simplify the necessary analysis, the thruster efficiency curve will be approximated by the straight line, $\eta_{MPD} = \alpha J - \theta$, where $\alpha = 1.5 \times 10^{-2} \text{kA}^{-1}$ and $\theta = 0.034$. For the time-varying discharge current supplied by the inductive storage system, the total thrust energy produced by the MPD thruster is given in terms of the efficiency:

$$E_{MPD} = \int_0^{\Delta T} JV\eta_{MPD}\,dt \tag{12}$$

For the inductive storage circuit, the thrust energy drops significantly as the minimum discharge current decreases because of the strong dependence of η_{MPD} on this current. To maximize this thrust energy, J_{min} must be as high as possible.

The total system efficiency is defined as the ratio of total thrust energy to the total energy supplied by the solar array power supply during the charge and discharge phases. The charging phase input energy and the discharge phase input energy are defined as

$$E_{ch} = \int_0^{T} J_{ch} V_{arr}\,dt \qquad E_{dis} = \int_0^{\Delta T} JV_{arr}\,dt \tag{13}$$

From Eqs. (12) and (13), the total system efficiency can be written as

$$\eta = E_{MPD}/(E_{ch} + E_{dis}) \tag{14}$$

By integrating the circuit equations developed in the previous section, analytic expressions for the energies in Eq. (14) can be obtained. These energies are all linearly dependent on ΔT; hence, the system efficiency is independent of this parameter. Total system efficiencies normalized to the maximum MPD thruster efficiency are shown in Figs. 9-11 vs J_{min} for various array powers and circuit resistances.

As can be seen in Fig. 10 for a fixed J_{min}, the system efficiency increases as the circuit resistance decreases. For a resistance of zero, the efficiency is a maximum. For this zero resistance case, as J_{min} increases, the average discharge current increases, and the increase in MPD thruster efficiency with current causes the system efficiency to increase to its maximum value. For larger values of resistance, increasing Ohmic losses counter the thruster efficiency increase and shift the maximum system efficiency to low values of J_{min}, as seen in Fig. 10 for $R = 0.18$ mΩ.

The competing effects of increasing thruster efficiency for higher J_{min} and decreasing Ohmic losses for lower J_{min}, force the system efficiency to a maximum value at either J_{min} close to zero or close to J_{max}. It is evident from Figs. 9-11 that there must exist a value of resistance at which the efficiency is essentially independent of J_{min}. This resistance is found where the efficiency for J_{min} close to J_{max} equals the efficiency for J_{min} close to zero. Setting these efficiencies equal to one another allows the development of an analytical expression for this resistance as a function of input power. Due to the complexity of this expression, only an approximate solution may be found, as shown in Fig. 12 as a cross-hatched line. Also shown in this figure is the linear expression between

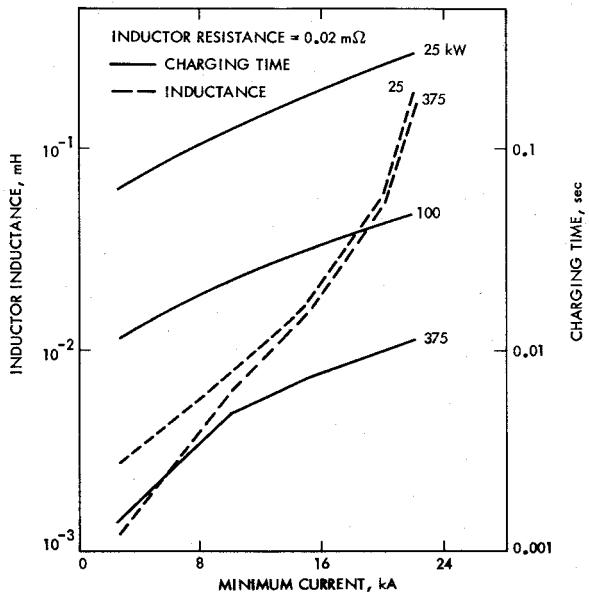

Fig. 7 Inductance and charging time for a fixed resistance.

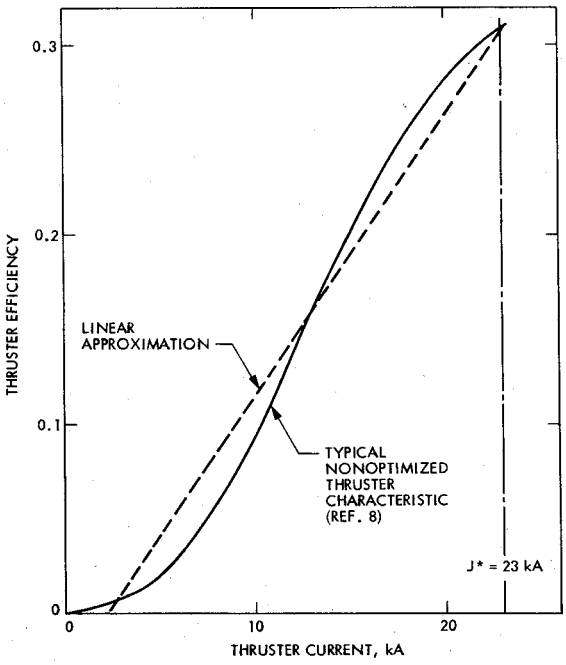

Fig. 8 MPD thruster efficiency.

power and circuit resistance given by Eq. (7), which demarks the value of maximum circuit resistance for a given power. For region I, the combination of array power and circuit resistance dictate that the maximum efficiency is attained for J_{min} approaching zero. In region II, the best system efficiency occurs for J_{min} approaching J_{max}. Referring back to Figs. 9-11, it can be seen that the best overall system efficiencies occur for small circuit resistance corresponding to region II of Fig. 12.

The variation in system efficiency is shown in Fig. 13 vs resistance for a fixed J_{min} near J_{max} for the power levels under consideration. At any circuit resistance, a larger array power gives a higher system efficiency due to shorter charging time and resulting lower Ohmic losses. As can be seen, for a given efficiency, the allowable resistance increases over a factor of ten as the power increases from 25 to 375 kW.

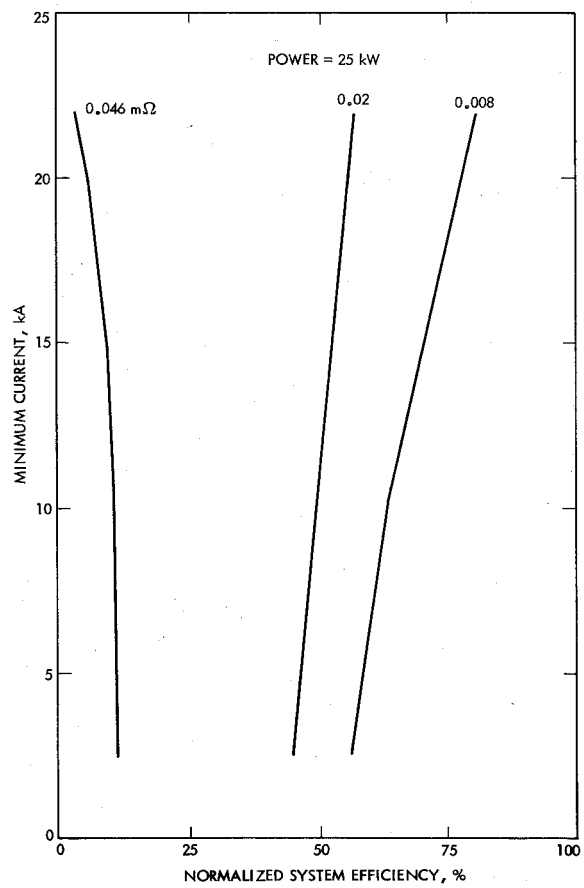

Fig. 9 Normalized total system efficiency, 25 kW.

Inductor Design

For any MPD thruster system, the final design choice depends not only on the total system efficiency, but also on the system mass. To date, little work has been done to characterize the mass of the MPD thruster; however, preliminary estimates by various investigators indicate that for an MPD thruster inductive energy storage system, excluding the solar array, the inductor mass will dominate.[6,11] This inductor must be designed to have a minimum mass, while meeting the required values of inductance and resistance that will give the best overall system efficiency.

The previous analysis indicates that the required inductance of the energy storage circuit is relatively insensitive to changes in input power or circuit resistance. The dependence of this inductance on J_{min} is relatively strong; however, for reasonable system efficiencies, this current is restricted to values close to J_{max}. Hence, an estimate of the minimum inductance required for acceptable system operation can be found. For this inductance, determining an accurate value of the minimum inductor mass requires a detailed development of the variation of this mass with coil configuration, conductor material and temperature, core material, and the allowable values of coil resistance for the various system solar array power levels. Rather than attempting such an analysis, a simple estimate of the coil minimum mass scaling with solar array power was made for a toroidal air-core inductor. Although this estimate is only for one particular type of coil, it is felt that the results are generally applicable to other coil designs.

Using known expressions for the mass, inductance and resistance of a toroidal coil, in terms of the number of turns in the coil, and the torus major and minor radii, the normalized minimum mass of the torus was found as a function of its

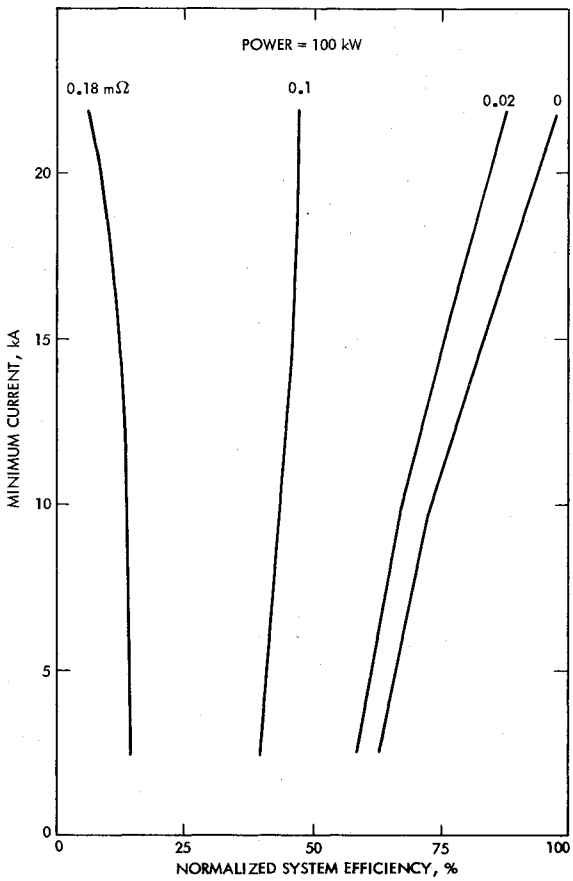

Fig. 10 Normalized total system efficiency, 100 kW.

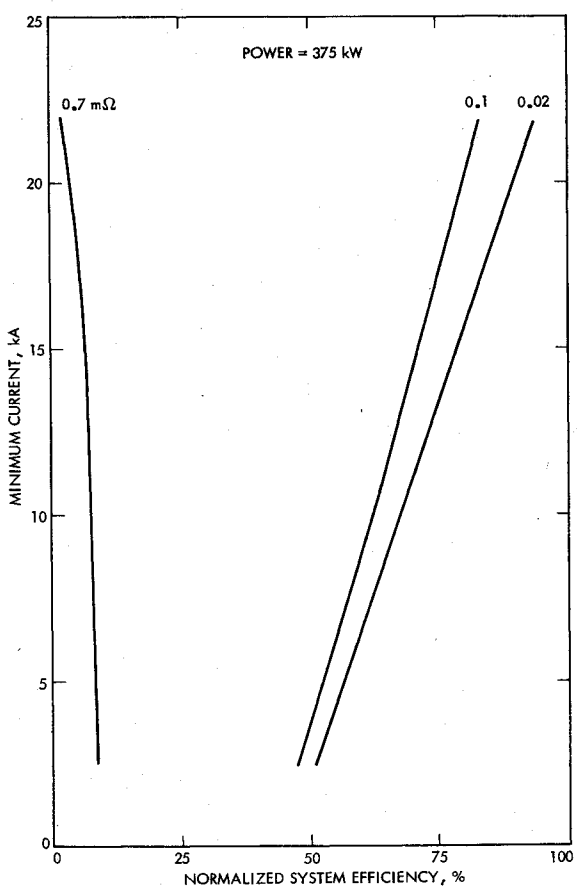

Fig. 11 Normalized total system efficiency, 375 kW.

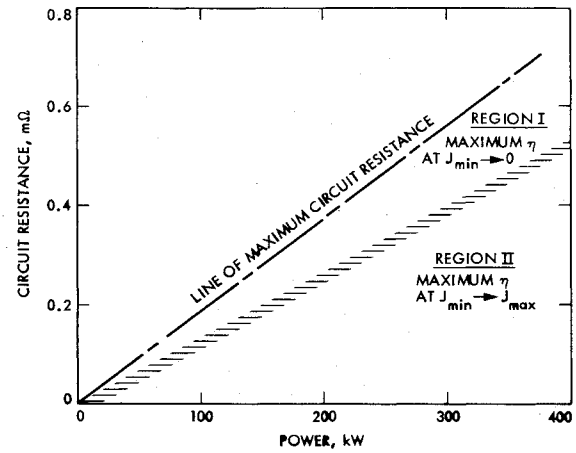

Fig. 12 Domain of optimum circuit operation.

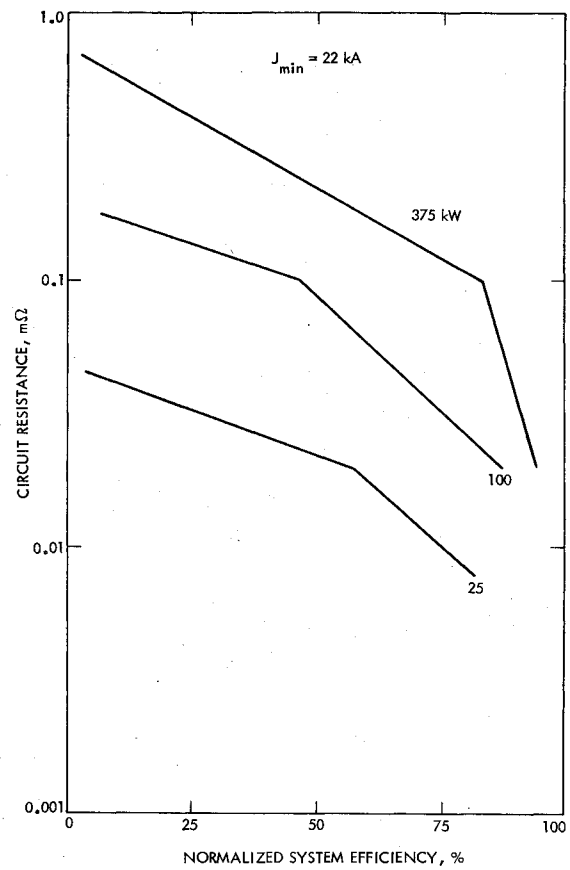

Fig. 13 Normalized total system efficiency vs circuit resistance.

resistance for a constant inductance. This relation indicates that to have a low mass coil, the coil resistance needs to be high. From the previous system circuit analysis, the total circuit resistance is fixed by J_{min}, P_{arr}, and the desired system efficiency. Under the most favorable conditions, the inductor resistance equals the total circuit resistance; hence, the inductor mass is related to the solar array power as shown in Fig. 14. As can be seen, the minimum inductor mass grows significantly as solar array power decreases. Previous studies have indicated that at a power level of 400 kW,[6] the inductor mass can be as high as 10^3 kg; hence from Fig. 14, the inductor mass at lower powers is likely to be prohibitively high.

These estimates of inductor coil masses have considered ordinary conductors with finite resistivities. To attain the

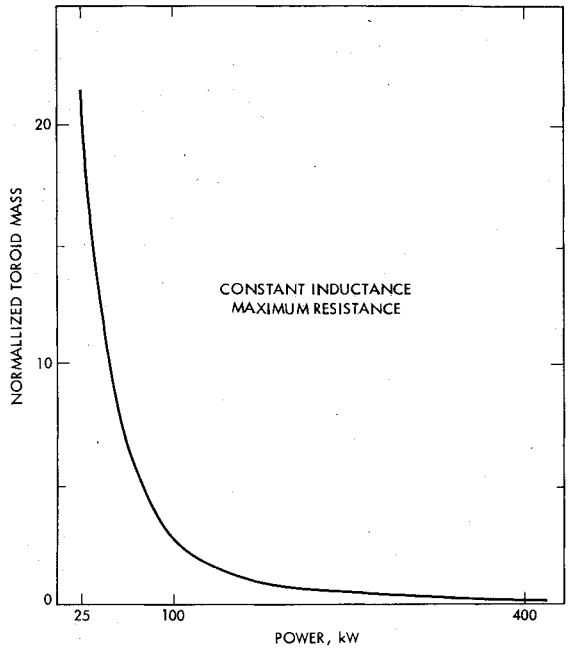

Fig. 14 Normalized inductor mass.

values of resistance required for the inductive storage system with these finite resistivities, large conductor volumes, and, hence, masses are required. One way of reducing these requirements is to reduce the conductor resistivity by using a superconducting energy storage coil. Various design studies of superconducting coils with characteristics similar to those required for the MPD thruster-inductive storage system indicate that the actual superconducting coil mass can be as low as 10 kg[12,13]; however penalties on both system mass and power are imposed by the added requirements for a cryogenic refrigerator and inductor dewar. Further work in this area is necessary before an accurate assessment of the characteristics of such an MPD thruster-cryogenic inductive storage system can be made.

Conclusion

Application of inductive energy storage to quasisteady MPD thruster systems is a relatively new concept that has thus far received attention only for a 400 kW nuclear power supply. This work considers an inductive system operated from a solar array at power levels of 25, 100, and 375 kW, in order to assess the particular advantages and disadvantages of this system when compared to alternative energy storage concepts. Using approximate expressions for the solar array and MPD thruster characteristics, the system circuit equations were solved. These solutions were then used to calculate the system efficiency for various operating conditions and to estimate the manner in which the mass of the inductor scaled with system power. While the results of this study allow initial conclusions on the application of inductive energy storage to MPD thruster systems, the use of a nonideal switch, the circuit component dynamic characteristics, other circuit configurations, and improved thruster power and efficiency levels must all be considered prior to any final resolution of the system characteristics.

This study represents the initial phase of an ongoing study of energy storage systems for MPD thrusters. Systems still to be studied include capacitive systems and inertial energy storage systems, which can be modeled as capacitive systems for circuit analysis. Combinations of capacitive and inductive elements, i.e., a pulse forming system, will also be addressed. Until these studies are complete, it will remain difficult to make any specific comparisons between these systems; however, some initial conclusions may be made. The sensitivity of the inductive storage system efficiency to circuit resistance is primarily due to the high currents involved in the circuit charging phase. Minimizing this resistance is apt to prove difficult for solar array power systems due to the large areas and long conductors required. This suggests that more compact power supplies such as nuclear systems might be favored. The ratio of Ohmic energy loss to thruster input energy increases at lower power levels, due to the longer inductor charging time, and leads to the observed inverse inductor mass scaling with input power. The higher voltages associated with capacitive energy storage systems would reduce these charging phase Ohmic losses since the average currents would be lower. Thus, at lower power levels, one would expect capacitive systems to be more efficient and less massive. At higher power levels, as the charging phase Ohmic losses become more significant, capacitive systems would become more massive in order to maintain reasonable efficiencies. Thus, for low powers capacitive energy storage would appear to be more desirable, while for higher powers inductive energy storage will be the better option due to its lower mass and higher efficiency.

Acknowledgments

This paper presents the results of one phase of research carried out at the Jet Propulsion Laboratory, California Institute of Technology under Contract No. NAS7-100 sponsored by the National Aeronautics and Space Administration.

References

[1] Jahn, R.G., *Physics of Electric Propulsion,* McGraw-Hill Book Co., New York, 1968.

[2] Malliaris, A.C., John, R.R., Garrison, R.L., and Libby, D.R., "Performance of Quasi-Steady MPD Thrusters at High Powers," *AIAA Journal,* Vol. 10, Feb. 1972, pp. 121-122.

[3] Saber, A.J. and Jahn, R.G., "Anode Power Deposition in Quasi-Steady MPD Arcs," AIAA Paper 73-1091, AIAA 10th Electric Propulsion Conference, Lake Tahoe, Nev., Oct.-Nov. 1973.

[4] Clark, K.E. and Jahn, R.G., "Quasi-Steady Plasma Acceleration," *AIAA Journal,* Vol. 8, Feb. 1970, pp. 216-220.

[5] Clark, K.E., "Inductive Storage for Quasi-Steady MPD Thrusters," AIAA Paper 78-654, AIAA/DGLR 13th International Electric Propulsion Conference, San Diego, Calif., April 1978.

[6] Britt, E.J., Clark, K.E., and Pawlik, E.V., "Inductively Coupled TI-MPD Spacecraft Electric Propulsion," *Proceedings of the 11th Intersociety Energy Conversion Engineering Conference,* Stateline, Nev., Sept. 1976, pp. 1471-1478.

[7] Boyle, M.J., Clark, K.E., and Jahn, R.G., "Flowfield Characteristics and Performance Limitations of Quasi-Steady Magnetoplasma Dynamic Accelerators," *AIAA Journal,* Vol. 14, July 1976, pp. 952-955.

[8] Rudolph, L.K., Jahn, R.G., Clark, K.E., and von Jaskowsky, W.F., "Performance Characteristics of Quasi-Steady MPD Discharges," AIAA Paper 76-1000, AIAA International Electric Propulsion Conference, Key Biscayne, Fla., Nov. 1976.

[9] Rudolph, L.K., Jahn, R.G., Clark, K.E., and von Jaskowsky, W.F., "Onset Phenomena in Self-Field MPD Arcjets," AIAA Paper 78-653, AIAA/DGLR 13th International Electric Propulsion Conference, San Diego, Calif., April 1978.

[10] Kuriki, K. and Suzuki, H., "Thrust Measurement of Quasi-Steady MPD Arcjet," AIAA Paper 76-1002, AIAA International Electric Propulsion Conference, Key Biscayne, Fla., Nov. 1976.

[11] Jahn, R.G. and Clark, K.E., "Energy Management Technology Forecast for Space Operations and Propulsion: Electromagnetic Accelerator," Jet Propulsion Laboratory, Pasadena, Calif., Rept. No. 1060-42, Vol. 4, Part 2, Jan. 1976, pp. 138-191.

[12] Teno, J., et al., "Development of a Pulsed High-Energy Inductive Energy Storage System," Air Force Aero Propulsion Lab., TR-73-49, Aug. 1973.

[13] Lucas, E.J., et al., "Design Construction and Testing of a Pulsed High Energy Inductive Superconducting Energy Storage System," Air Force Aero Propulsion Laboratory, TR-75-60, Sept. 1975.